

Supplementary Materials

Hierarchical core/shell meso-ZSM-5@mesoporous aluminosilicate-supported Pt
nanoparticles for bifunctional hydrocracking

Darui Wang, Le Xu, Peng Wu*

*Shanghai Key Laboratory of Green Chemistry and Chemical Processes, Department
of Chemistry, East China Normal University, North Zhongshan Rd. 3663, Shanghai
200062, P. R. China*

E-mail: pwwu@chem.ecnu.edu.cn

Tel/Fax: 86-21-62232292

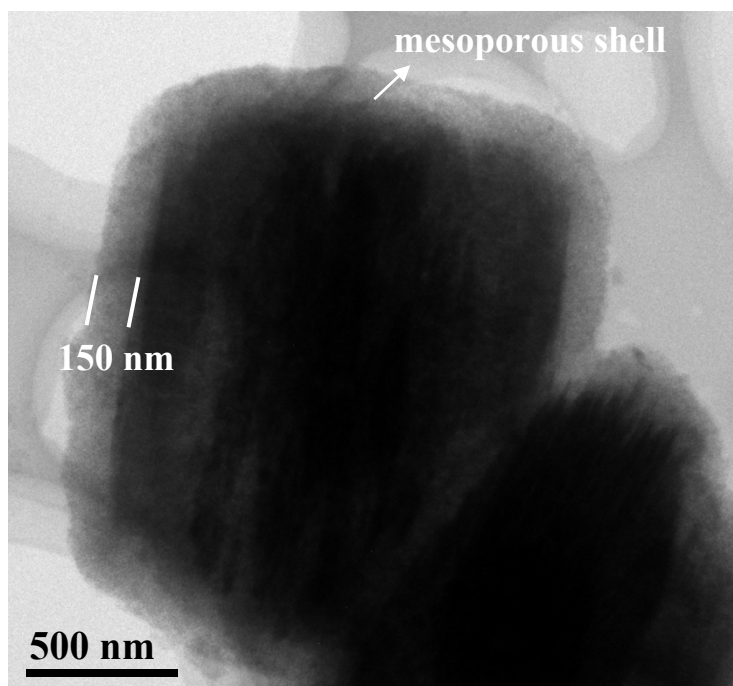


Fig. S1 TEM image of core-shell structured $MZ_{AT0.2-PI0.02}@MSA$, showing a uniform core-shell structure with a shell thickness of 150 nm.

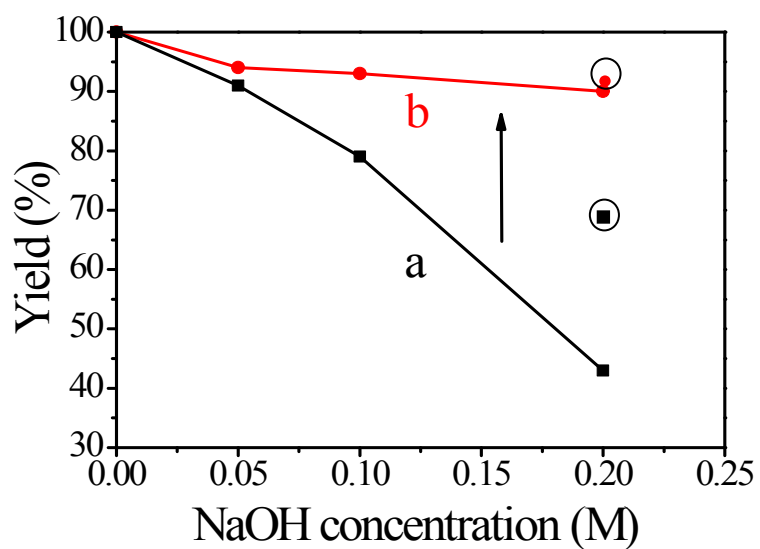


Fig. S2 Dependence of product yield on NaOH concentration for MZ_x samples (a) and core-shell structured composite materials $MZ_x@MSA$ (b). The yield is defined as grams of solid after workup per gram of ZSM-5 used. Circled points represent $MZ_{AT0.2-Pi0.02}$ and $MZ_{AT0.2-Pi0.02}@MSA$ both synthesized by desilication with 0.2 M NaOH in the presence of piperidine.

Table S1 Acidity properties and Si/Al molar ratios of different samples

No.	Samples	Si/Al ^a	Q ^b (mmol g ⁻¹)		
			Weak	Strong	Total
1	ZSM-5	38	0.19	0.28	0.47
2	MZ _{AT0.2-PI0.02}	28(63 ^c)	0.26	0.24	0.50
3	MZ _{AT0.2-PI0.02} @MSA	36	0.14	0.21	0.35
4	MZ _{AT0.2-PI0.02} &MSA	35	0.14	0.22	0.36
5	MSA	61	0.06	-	0.06

^a Si/Al molar ratios measured by ICP. ^b Acidity determined by NH₃-TPD

measurement. ^cThe Si/Al molar ratio of the filtrate obtained from MZ_{AT0.2-PI0.02}.

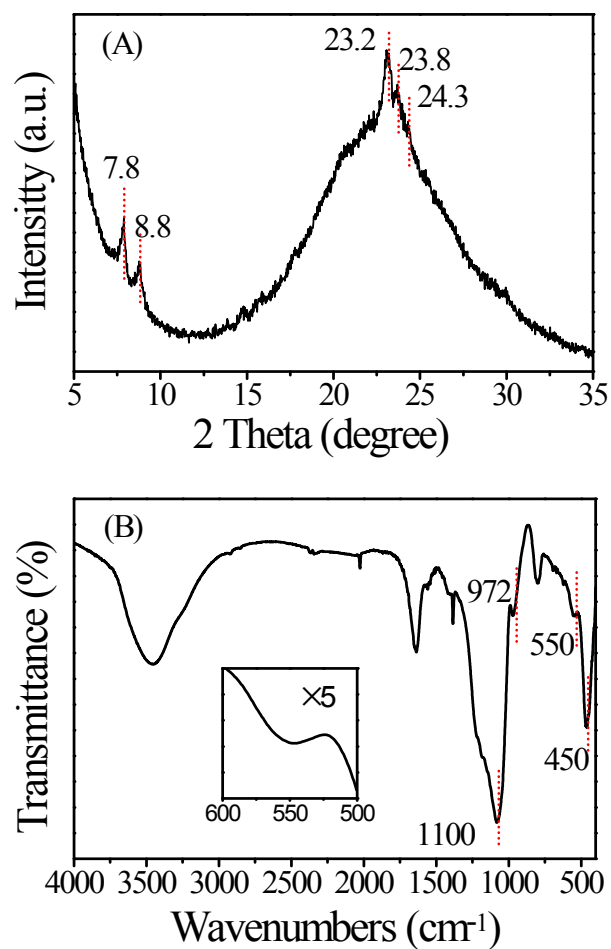


Fig. S3 XRD pattern (A) and FT-IR spectrum (B) of the MSA material. The pure Al-containing mesoporous silica was self-assembled from the filtrate of ZSM-5 desilication.

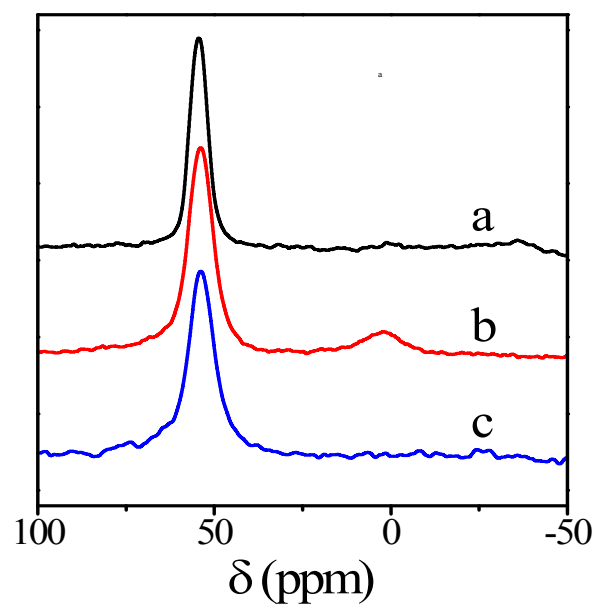


Fig. S4 ^{27}Al MAS NMR spectra of ZSM-5 (a), $\text{MZ}_{\text{AT}0.2\text{-PI}0.02}$ (b), $\text{MZ}_{\text{AT}0.2\text{-PI}0.02}\text{@MSA}$ (c).

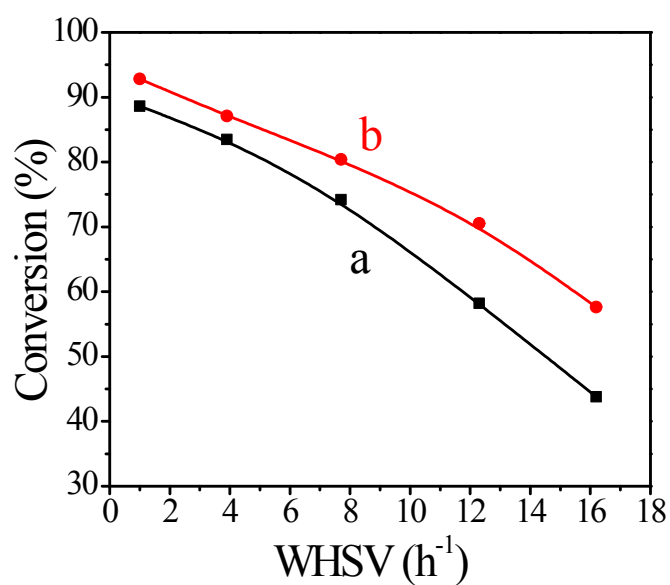


Fig. S5 The dependence of *n*-hexadecane conversion on space velocity in the hydrocracking over Pt/ZSM-5 (a) and Pt/MZ_{AT0.2}-Pt_{0.02}@MSA (b). Reaction conditions: catalyst, 0.1 g; WHSV, 1 ~ 16.2 h⁻¹; H₂:C₁₆ molar ratio, 35; temperature, 573 K; atmospheric pressure. The WHSV was varied by changing the flow rate of C₁₆ from 0.1 to 1.62 g h⁻¹.

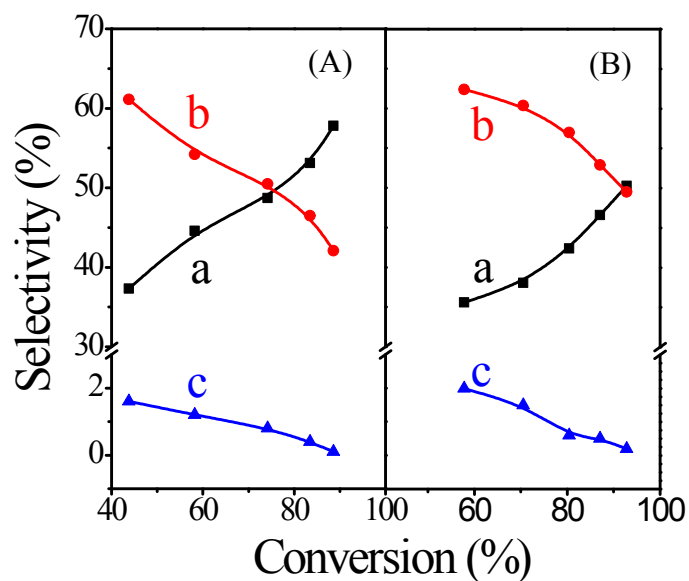


Fig. S6 The dependence of product selectivity on the *n*-hexadecane conversion of hydrocracking over Pt/ZSM-5 (A) and Pt/MZ_{AT0.2-P10.02}@MSA (B). (a) C₁ - C₄ selectivity (a), (b) C₅ - C₁₁ selectivity, and C₁₂ - C₁₅ selectivity. Reaction conditions: catalyst, 0.1 g; WHSV, 1 ~ 16.2 h⁻¹; H₂:C₁₆ molar ratio, 35; temperature, 573 K; atmospheric pressure. The WHSV was varied by changing the flow rate of C₁₆ in the range of 0.1 - 1.62 g h⁻¹.

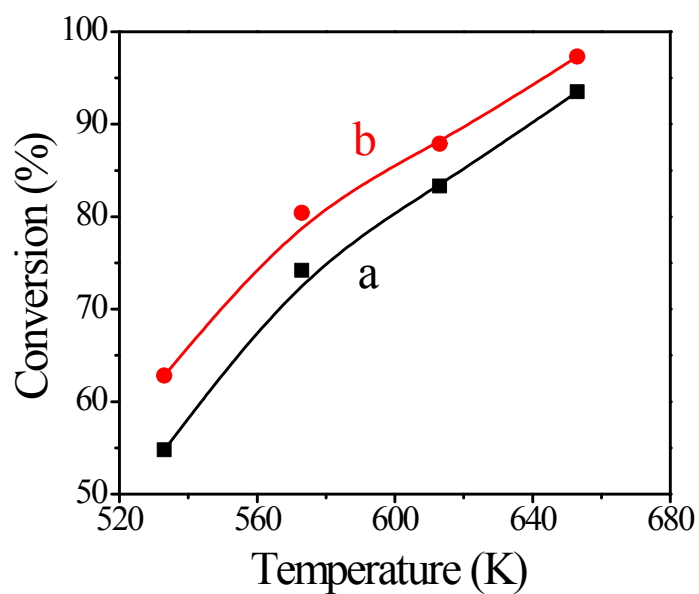


Fig. S7 The dependence of *n*-hexadecane conversion in the hydrocracking of over Pt/ZSM-5 (a) and Pt/MZ_{AT0.2-PI0.02}@MSA (b). Reaction conditions: catalyst, 0.1 g; WHSV, 7.7 h⁻¹; H₂:C₁₆ molar ratio, 35; H₂ flow rate, 45 mL min⁻¹; temperature, 533 ~ 653 K; atmospheric pressure.

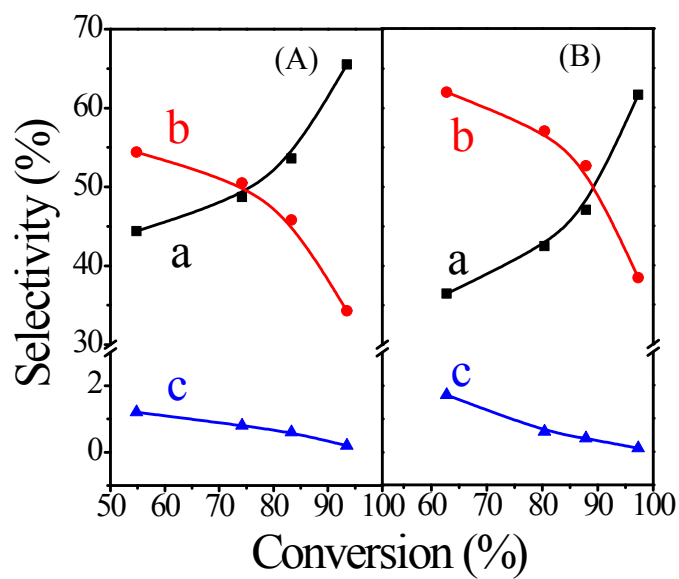


Fig. S8 The dependence of product selectivity on the *n*-hexadecane conversion of hydrocracking over Pt/ZSM-5 (A) and Pt/MZ_{AT0.2-P10.02}@MSA (B). (a) C₁ - C₄ selectivity (a), (b) C₅ - C₁₁ selectivity, and C₁₂ - C₁₅ selectivity. Reaction conditions: catalyst, 0.1 g; WHSV, 7.7 h⁻¹; H₂:C₁₆ molar ratio, 35; H₂ flow rate, 45 mL min⁻¹; temperature, 533 ~ 653 K; atmospheric pressure.